7. C. Dreller, *Behav. Ecol. Sociobiol.* **43**, 191 (1998).
8. J. B. Becker, R. L. Meisel, *Handbook of Neurochemistry and Molecular Neurobiology: Behavioral Neurochemistry, Neuroendocrinology and Molecular Neurobiology* (Springer, New York, 2007).
9. D. Viggiano, D. Vallone, H. Welzl, A. G. Sadile, *Behav. Genet.* **32**, 315 (2002).
10. R. P. Ebstein *et al.*, *Nat. Genet.* **12**, 78 (1996).
11. J. Benjamin *et al.*, *Nat. Genet.* **12**, 81 (1996).
12. J. A. Mustard *et al.*, *Brain Res. Mol. Brain Res.* **113**, 67 (2003).
13. P. D. Evans, B. Maqueira, *Invert. Neurosci.* **5**, 111 (2005).
14. F. W. Schürmann, K. Elekes, M. Geffard, *Cell Tissue Res.* **256**, 399 (1989).
15. G. Bicker, S. Schäfer, O. P. Ottersen, J. Storm-Mathisen, *J. Neurosci.* **8**, 2108 (1988).
16. R. Kucharski, E. E. Ball, D. C. Hayward, R. Maleszka, *Gene* **242**, 399 (2000).
17. P. T. Kurshan, I. S. Hamilton, J. A. Mustard, A. R. Mercer, *J. Comp. Neurol.* **466**, 91 (2003).
18. A. Bendesky, M. Tsunozaki, M. V. Rockman, L. Kruglyak, C. I. Bargmann, *Nature* **472**, 313 (2011).

Acknowledgments: Special thanks to M. K. Carr-Markell and J. Recchia-Rife for extensive help in the field. We also thank the following: C. Nye and K. Pruiett (bee management); A. Brockmann, P. Date, J. Dotterer, L. Felley, M. Girard, S. Kantarovich, H. S. Pollock, and M. Wray (field assistance); T. Newman (molecular studies); S. Aref and A. Toth (statistics); E. Hadley (graphics); and A. M. Bell, D. F. Clayton, R. C. Fuller, J. S. Rhodes, C. W. Whitfield, and members of the Robinson laboratory (review of the manuscript). Supported by NSF Frontiers in Biological Research grant EF 0425852 (B. L. Schatz, PI, BeeSpace Project); NIH Director's Pioneer Award 1DP1OD006416 (G.E.R); and the Illinois Sociogenomics Initiative (G.E.R). Microarray data meet Minimum Information About Microarray Experiment (MIAME) standards and are available at ArrayExpress (www.ebi.ac.uk/arrayexpress, #E-MTAB-491). Z.S.L. and G.E.R. conceived the project, designed the experiments and wrote the paper; Z.S.L. performed sample collection, molecular and field experiments, and analyses; T.N. and S.L.R.-Z. performed microarray experiments and statistical analyses, respectively; and H.R.M. and T.D.S. contributed to protocol development and sample collection and co-wrote the paper.

Supporting Online Material

www.sciencemag.org/cgi/content/full/335/6073/1225/DC1
Materials and Methods
SOM Text
Figs. S1 to S8
Tables S1 to S6
References

14 September 2011; accepted 1 February 2012
10.1126/science.1213962

Atomic View of a Toxic Amyloid Small Oligomer

Arthur Laganowsky,[1]* Cong Liu,[1] Michael R. Sawaya,[1] Julian P. Whitelegge,[2] Jiyong Park,[1] Minglei Zhao,[1] Anna Pensalfini,[3] Angela B. Soriaga,[1] Meytal Landau,[1] Poh K. Teng,[1] Duilio Cascio,[1] Charles Glabe,[3] David Eisenberg[1]†

Amyloid diseases, including Alzheimer's, Parkinson's, and the prion conditions, are each associated with a particular protein in fibrillar form. These amyloid fibrils were long suspected to be the disease agents, but evidence suggests that smaller, often transient and polymorphic oligomers are the toxic entities. Here, we identify a segment of the amyloid-forming protein αB crystallin, which forms an oligomeric complex exhibiting properties of other amyloid oligomers: β-sheet–rich structure, cytotoxicity, and recognition by an oligomer-specific antibody. The x-ray–derived atomic structure of the oligomer reveals a cylindrical barrel, formed from six antiparallel protein strands, that we term a cylindrin. The cylindrin structure is compatible with a sequence segment from the β-amyloid protein of Alzheimer's disease. Cylindrins offer models for the hitherto elusive structures of amyloid oligomers.

Studies from many laboratories have suggested that the molecular agents in amyloid-related conditions are not the associated protein fibrils that have long been taken as the defining feature of these disorders but instead are lower molecular weight entities, often termed small amyloid oligomers (*1*–*7*). These oligomers are not generally stable aggregates; they appear as transient species during the conversion of their monomeric precursors to more massive, stable fibrils, and sometimes they appear as an ensemble of sizes and shapes. This polymorphic and time-dependent nature of small amyloid oligomers has made it difficult to pin down their assembly pathways, their stoichiometries, their atomic-level structures, their relationship to fibrils, and their pathological actions (*1*, *8*–*10*). What has emerged is a consensus, minimal definition of small amyloid oligomers: They are noncovalent assemblies of several identical chains of proteins also known to form amyloid fibrils; the oligomers exhibit greater cytotoxicity than either the monomer or fibrils formed from the same protein; in many cases, the oligomer is recognized by a "conformational" antibody (A11) that binds oligomers but not fibrils, regardless of the sequence of the constituent protein (*5*). This suggests that oligomers display common conformation features that differ from those of fibrils (*11*).

In seeking to better define small amyloid oligomers, we chose to work with αB crystallin (ABC). This protein is a chaperone (*12*–*14*) that forms amyloid fibrils (*15*), but the fibrils form more slowly than those of the β-amyloid peptide (Aβ) or islet amyloid polypeptide (IAPP), so that the oligomeric state may be trapped before the onset of fibrillization. We have identified a segment of ABC that forms a relatively stable small oligomer, which satisfies the definition of a small amyloid oligomer given in the preceding paragraph.

We identified the oligomer-forming segment of ABC by inspection of its three-dimensional (3D) structure (*16*) and by applying the RosettaProfile algorithm to its sequence. This algorithm identifies sequence segments that form the steric-zipper spines of amyloid fibrils (*17*, *18*). We noted that two segments of high amyloidogenic propensity, with sequences KVKVLG and GDVIEV (where D indicates Asp; E, Glu; G, Gly; I, Ile; K, Lys; and V, Val), share the same Gly residue 95 at the C terminus of the first segment and the N terminus of the second; moreover, the entire 11-residue segment KVKVLGDVIEV forms a hairpin loop in the 3D structure of ABC (Fig. 1A), with Gly at its center. As predicted, the second six-residue segment GDVIEV, termed G6V (Table 1 defines the structures described in this report), forms fibrils and microcrystals (fig. S1). The microcrystals enabled us to determine the atomic structure of G6V (fig. S2), which proved to be a standard class 2 steric zipper (*19*), essentially an amyloid-like protofilament.

The hairpin segment KVKVLGDVIEV (termed K11V) formed both amyloid fibrils and oligomers. Upon shaking at elevated temperature, K11V forms fibrils similar to those of the parent protein (ABC) from which the segment is derived (*15*) and similar to those of a tandem repeat of $K11V^{V2L}$ (K11V-TR, see below) (Fig. 1B; fig. S1, B and C; and table S1). The fibrils range from 20 to 100 nm in diameter as viewed by electron microscopy (fig. S1). X-ray diffraction of dried fibrils displayed rings at 4.8 and 12 Å resolutions, consistent with the signature cross-β pattern of amyloid fibrils (fig. S1C). The amyloid fibrils of K11V-TR bind the specific amyloid dye congo red, producing apple-green bifringerance under polarized light (fig. S1D), and are immunoreactive with the fibril-specific, conformation-dependent antibody OC (Fig. 1E) (*20*). Together these results prove that the segments G6V, K11V, and K11V-TR are all capable of converting to the amyloid state (*21*, *22*), as is their parent protein, ABC.

Under physiological conditions, the segments K11V, K11V-TR, and a sequence variant with Leu replacing Val at position 2 ($K11V^{V2L}$) all form stable small oligomers intermediate in size

[1]Department of Biological Chemistry and Department of Chemistry and Biochemistry, University of California Los Angeles (UCLA), Howard Hughes Medical Institute (HHMI), UCLA-DOE Institute for Genomics and Proteomics, Los Angeles, CA 90095, USA. [2]The Neuropsychiatric Institute (NPI)–Semel Institute for Neuroscience and Human Behavior, UCLA, Los Angeles, CA 90024, USA. [3]Department of Molecular Biology and Biochemistry, University of California, Irvine, CA 92697, USA.

*Present address: Department of Chemistry, Chemistry Research Laboratory, University of Oxford, Oxford, UK.
†To whom correspondence should be addressed. E-mail: david@mbi.ucla.edu

between monomer and fiber. For each sequence, we determined the number of molecules in the oligomers by size-exclusion high-performance liquid chromatography (SEC-HPLC) and native mass spectrometry experiments. Purified recombinant K11V^{V2L} and K11V-TR, a tandem repeat of K11V^{V2L}, eluted as oligomeric complexes by SEC (Fig. 1C). For example, the K11V-TR complex was estimated to be ~8 kD in mass, corresponding roughly to three tandem segment chains. As an additional check on the stoichiometry of the tandem repeat K11V-TR oligomer, we subjected peak fractions to native nanoelectrospray mass spectrometry. Mass spectra showed abundant ions of K11V-TR oligomers with masses corresponding to three peptide chains (Fig. 1D and fig. S3). Furthermore, we were able to isolate ions of the K11V-TR oligomer and perform collision-induced dissociation (CID) of this trimeric peptide complex into monomeric units of mass equal to that of the K11V-TR peptide (fig. S4). Similar experiments show that K11V and K11V^{V2L} form hexameric oligomers (Table 1 and fig. S3). Thus, native mass spectrometry is consistent with SEC-HPLC in suggesting a stoichiometry of a K11V oligomer of six chains and a K11V-TR oligomer of three tandem chains. These results are consistent with crystallography and energetic considerations (see below).

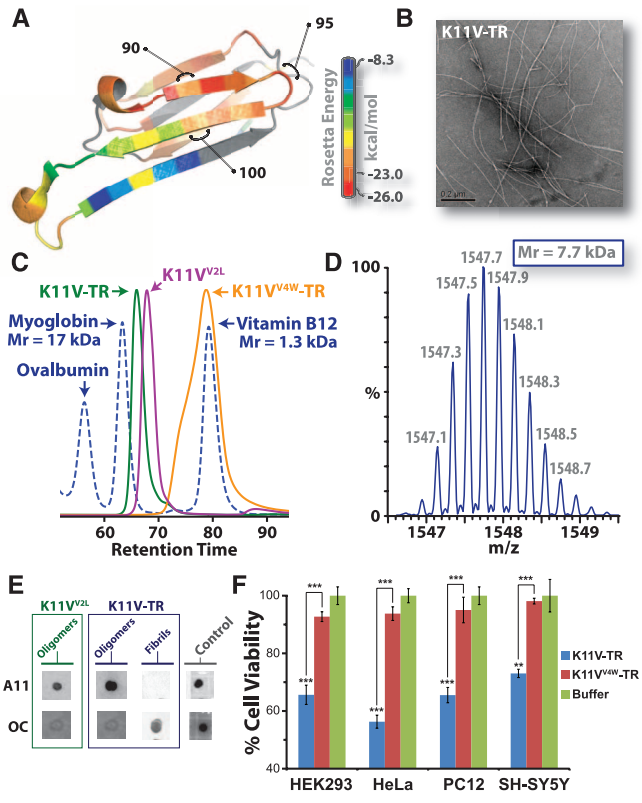

Fig. 1. The cylindrins derived from ABC, an amyloid-forming protein, exhibit the properties of oligomeric state, immunoreactivity, and cytotoxicity commonly ascribed to small amyloid oligomers. (**A**) Ribbon diagram of a single subunit of ABC (*16*), colored by propensity to form amyloid, with red being the highest and blue the lowest propensity. The segment from residue 90 to 100, termed K11V, forms the cylindrin. (**B**) Representative electron micrograph of amyloid fibrils formed by K11V-TR. (**C**) Overlaid size-exclusion chromatograms showing protein standards (blue dashed curve) and cylindrin segments. K11V^{V2L} (purple curve; 1.2 kD per chain) and K11V-TR (green curve; 2.5 kD per chain) cylindrin segments migrate as oligomeric complexes. A mutant form of K11V-TR that disrupts oligomer formation of the cylindrin peptide, K11V^{V4W}-TR (orange curve; 2.7 kD per chain), migrates as a dimeric or monomeric species. (**D**) Native nanoelectrospray mass spectrum of K11V-TR peak fractions from SEC-HPLC reveals trimeric tandem-repeat cylindrin oligomers, confirming that the oligomeric complexes coincide in mass with the crystallized cylindrins. Expansion of the most abundant ion series of a +5 charge state corresponding to a molecular mass of three K11V-TR chains, coinciding with the crystallographic trimeric oligomer with a mass accuracy of 3.93 parts per million (ppm), is shown, with mass/charge (*m/z*) labels. (**E**) Immunodot blot analysis of solutions of K11V^{V2L} and K11V-TR oligomers and K11V-TR fibrils with prefibrillar oligomer-specific, polyclonal antibody A11 (*5*); and a mixture of fibril-specific monoclonal antibodies, OC (*11*). Solutions of cylindrin-forming segments are recognized by A11 but not by the OC antibody. In contrast, K11V-TR fibrils are recognized only by the OC antibody. Positive controls are shown to the right (*5*). (**F**) Cylindrin K11V-TR is toxic to four mammalian cell lines. Cell viability levels return to nearly 100% when we tested the control variant K11V^{V4W}-TR. All samples were at a final concentration of 100 μM. Results represent mean ± SEM. Student's *t* test ($N = 4$): $^{**}P < 0.01$; $^{***}P < 0.001$.

These ABC K11V oligomers exhibit molecular properties in common with amyloid oligomers from other disease-related proteins. We probed blots of the recombinant segments with the polyclonal A11, amyloid-oligomer–specific conformational antibody (*5*). Both single and tandem repeat segments are recognized by the A11 antibody (Fig. 1E and fig. S1E). By using a cell viability assay on mammalian cells, we observed oligomers to be toxic, displaying dose-response effects similar to those of Aβ involved in Alzheimer's disease (*2*, *23*, *24*) (Fig. 1F and fig. S5). To test whether membrane disruption is responsible for this toxicity, as suggested for human islet amyloid polypeptide (hIAPP) (*25*, *26*), we performed liposome dye release experiments. The hIAPP peptide diminished liposome integrity leading to dye release, but the K11V-TR did not exhibit this trend (fig. S6). In contrast to oligomeric solutions, no toxicity was observed for the fibrils of G6V. Thus, ABC segments in oligomeric form are cytotoxic but suggest a more complicated mechanism of toxicity than membrane disruption.

Table 1. Structures and stoichiometries of amyloid-related oligomers discussed in this report, derived from ABC. Peptide segment amino acid sequences are provided in table S1. A dash entry indicates sample was not tested or unknown. MS, native mass spectrometry.

Protein/peptide segment (residue numbers)	Structure	PDB ID	Oligomer size by			Immunoreactivity	Toxicity
			Crystallography	SEC	MS		
ABC truncated (68–162)	Network of dimers linked by domain swapping	3L1G	2 to indefinitely large	2–4*	2–6 and 10–24*	–	No†
K11V	Cylindrin	3SGO	6	–	6‡	–	–
K11V^{V2L}	Cylindrin V2L variant	3SGP	6	6	6‡	A11	Yes
K11V-TR	Cylindrin tandem repeat V2L variant	3SGR	3	3	3‡	A11	Yes
K11V^{V4W}-TR	Cylindrin tandem repeat V2L/V4W variant	–	–	1–2	–	No§	No
G6V	Fibril steric zipper	3SGS	Indefinitely large	–	–	No	No

*Data refer to truncated ABC (*16*). †Data refer to full-length ABC (*50*). ‡Data shown in fig S3. §Very weak binding. Data shown in fig. S1E.

We next determined the crystal structures of various ABC K11V oligomers. A screen produced x-ray–grade crystals of K11V, but structure determination by molecular replacement with fiberlike probes failed, suggesting that the ABC segment oligomers possess a previously unobserved type of amyloid structure. Turning to the single-wavelength anomalous dispersion method for phase determination, we synthesized K11V derivatives with Br substitutions at position 2 or 8 of the K11V sequence, K11V-Br2 and K11V-Br8, with the leucine-resembling nonnatural amino acid (2-bromoallyl)-glycine. Both derivatives crystallized and led to structure determinations (table S2) at 1.4 Å resolution. Molecular replacement based on these structures led to the closely related structures of K11V itself as well as K11V-TR and $K11V^{V2L}$.

The structure of K11V, the amyloid-related oligomer, is a six-stranded antiparallel barrel of cylindrical shape, consistent in mass with our solution studies, that we term a cylindrin. The cylindrin (Fig. 2) is distinctly different in structure from either the native structure of ABC (Fig. 1A) or from its G6V segment (fig. S2), a dual β-sheet steric zipper. It is also distinct from other structures currently in the Protein Data Bank (PDB) (SOM text) but resembles several previously proposed β-barrel models (*27*–*31*). Each strand of the cylindrin is bonded to one neighboring strand by a strong interface and to a second by a weak interface. The strong interface (between purple and green chains, Fig. 2, B and C) is formed by 12 hydrogen bonds and splays outward at the ends. The weak interface is formed by eight hydrogen bonds: four from the main chain, two mediated through side-chain interactions, and two through a water bridge (Fig. 2C). The axial channel of the cylindrin is closed by the hydrophobic interactions of two inward-pointing sets of three valine side chains and is devoid of water (Fig. 2C). The surface area buried (A_b) per residue in the strand-packing interface of the cylindrin is 87 $Å^2$, smaller than the 131 $Å^2$ value for the strand-to-strand interface of the steric zipper of GNNQQNY (N, Asn; Q, Gln; and Y, Tyr) (*32*). Similarly the cylindrin-packing interface has a shape complementarity (*Sc*) value of 0.75, somewhat smaller than the value of 0.80 for the GNNQQNY interface (table S3). Thus, the cylindrin structure has features in common with a steric zipper in being formed from hydrogen-bonded β strands and having a dry interior, but it is cylindrical rather than nearly flat and is probably less stable, as suggested by the lower A_b and *Sc* values.

To provide adequate cylindrin material for biochemical and toxicological studies, we generated a synthetic gene to express in bacteria a tandem repeat, K11V-TR, of the well-diffracting $K11V^{V2L}$ segment, covalently linked through a double glycine linker and containing an additional N-terminal glycine (fig. S7 and table S1). This K11V-TR peptide reduces the complexity of the cylindrin assembly process from six to three chains (Fig. 2, D and E). We were able to determine the K11V-TR crystal structure, even though the glycine linkers produce some disorder in the crystals (table S2). Other than the glycine linkers and the Val-to-Leu replacement, the cylindrical bodies of the six-stranded K11V and the three double-stranded K11V-TR oligomers are essentially identical. Energetic considerations suggest that the cylindrin should be stable in solution: The surface area buried per interchain interface of K11V-TR is 841 $Å^2$, nearly as much as for the foldon trimerization domain, 1092 $Å^2$ (PDB 1RFO), and cylindrin forms twice as many hydrogen bonds

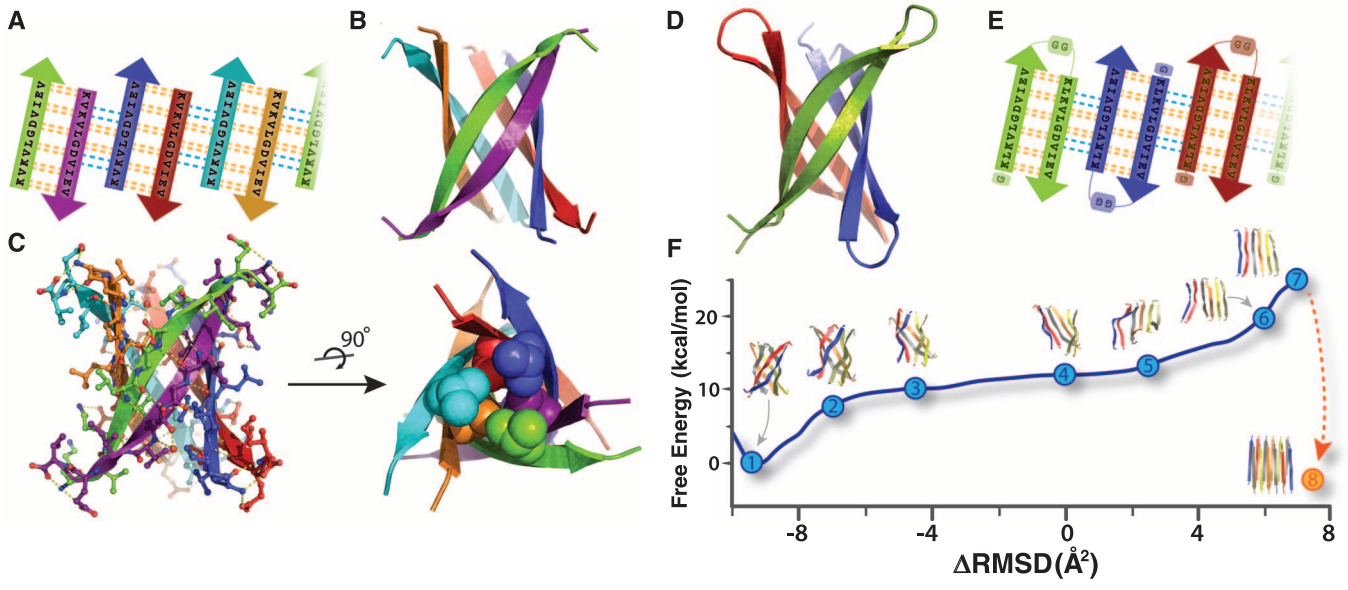

Fig. 2. Crystal structures of cylindrins and computed free energy change of the simulated structural transition from cylindrin to a fibril. Each colored β strand (arrow) is composed of 11 amino acid residues from ABC of sequence KVKVLGDVIEV (K11V). (**A**) Schematic of unrolled cylindrin (outside view), illustrating strand-to-strand registration. Hydrogen bonds between the main chains of neighboring strands are shown by yellow dashed lines; hydrogen bonds mediated by water bridges or side chains are shown by blue dashed lines. (**B**) Ribbon representation of the cylindrin crystal structure. Pairs of strands form antiparallel dimers, which assemble around a threefold axis down the barrel axis of the cylindrin. The height of the cylindrin is 22 Å. The inner dimension of the cylindrin, around the waist from Cα to Cα, is 12 Å, and at the splayed ends the diameter is 22 Å. (**C**) The cylindrin with side chains shown as atoms and hydrogen bonds in yellow. Twelve backbone hydrogen bonds stabilize the strong interface between tightly twisted antiparallel strands (e.g., between green and purple chains). The weaker interface between the pairs of tightly twisted strands is formed by four main-chain hydrogen bonds, with an additional two hydrogen bonds coming from a water bridge and two hydrogen bonds from side-chain interactions (e.g., between purple and blue chains). The dry interior of the cylinder is closed by triplets of Val residues, shown as spheres, at the top and bottom. (**D**) Crystal structure of K11V-TR formed by three chains of 25 residues each. (**E**) Schematic of unrolled K11V-TR cylindrin (outside view). Similar hydrogen-bonding patterns are formed as in (A). (**F**) The computed Gibbs free energy at 300 K for a cylindrin forced to a fibril. The reaction coordinate measures the difference in root mean square deviation (ΔRMSD) from the two end points: the cylindrin and the in-register antiparallel β sheet (IAB). The cylindrin set the free energy minimum (point 1). The transition was initiated by disrupting the weak interface (points 2 and 3). As the cylindrin unrolls, the weak interface requires complete dissociation of backbone hydrogen bonds (points 4 and 5), whereas the strong interfaces maintains hydrogen bonding (point 6). The IAB has a higher free energy than the cylindrin (point 7), and when two IABs associate and interdigitate to form a steric zipper (point 8) the free energy drops to 5.2 kcal/mol per peptide lower than the cylindrin (table S4).

between neighboring chains as does the foldon domain.

For a negative control of cylindrin structure and properties, we generated a variant form of the tandem segment, K11V^{V4W}-TR in which the V4W substitution occurs in both repeats (table S1). This substitution was predicted on the basis of the K11V crystal structure to disrupt oligomer formation through steric clash of core, buried residues. This variant peptide eluted in the mass range of a dimeric or monomeric species by SEC-HPLC and displayed reduced cell toxicity (Fig. 1F and fig. S5).

To compare cylindrins to fibers, we define a cylindrin as a toxic, amyloid-related, oligomeric, cylindrically shaped β barrel formed from antiparallel, extended protein strands and having the cylinder filled with packed side chains. A cylindrin resembles a steric zipper in having a packed interior but differs from a steric zipper in an important respect, which may illuminate the reaction pathway from oligomers to fibrils. When unrolled into a β sheet, each antiparallel pair of strands in the cylindrin sheet (Fig. 2A) is out of register with neighboring pairs by six residues (shear number is six) (fig. S8) (*33*). In contrast, the β strands in full amyloid fibers (*22*, *34*, *35*) and short steric zippers (*19*) are in register. This means that a cylindrin unrolled into a sheet would not be an in-register structure, ready to bond with an identical sheet to form the steric zipper spine of an amyloid fiber. The transition from cylindrin to steric zipper involves breaking of hydrogen bonds and re-registration of the strands into an in-register structure, as we have simulated by targeted molecular dynamics, followed by free energy perturbation in explicit solvent (Fig. 2F and SOM text). We chose the end target as an antiparallel sheet, on the basis of Fourier transform infrared (FTIR) experiments (SOM text). These calculations suggest that the transition from cylindrin to an antiparallel fiberlike structure involves crossing a high free energy, implying that fibers may nucleate from monomers without passing through cylindrin-like oligomeric states (*36*–*38*); that is, cylindrin is likely to be off pathway to fiber formation.

An important question is whether the ABC cylindrin is a possible model for amyloid oligomers formed by well-studied toxic proteins, such as Aβ and hIAPP. There is evidence that amyloid oligomers share common structural features. For example, studies have suggested oligomers are β-sheet rich (*38*–*40*), and several toxic oligomers are recognized by the A11 conformational antibody (*41*), which also recognizes the cylindrin. A11 also recognizes α-hemolysin, a soluble β-barrel protein (*42*). Thus, the cylindrin structure may represent the common structural core of amyloid oligomers (SOM text). To investigate this possibility, we used the Rosetta-Profile method (*18*) to ask whether other toxic sequences, or segments of them, are compatible with the cylindrin structure. We found that the C-terminal segment of Aβ is reasonably compatible with the cylindrin structure and, with a two-residue registration shift between pairs of antiparallel strands, a very good fit with the cylindrin structure is obtained (fig. S11). This finding in itself does not imply that this is the structure of the Aβ toxic species, but it is in agreement with the observation of hexamers of Aβ oligomers by native mass spectrometry analysis (*43*).

The ABC cylindrin may represent one of many possible assemblies of cylindrin-like structures. The number of strands or shear number may vary. For example, Aβ oligomers have been described ranging in size from dimers and tetramers to hexamers and dodecamers (*43*–*45*). Those with larger numbers of strands could have open central channels as modeled by others (*46*, *47*), whereas cylindrins having smaller numbers of strands would have dry interfaces similar to crystallographically (*48*, *49*) and computationally (*44*) derived models. Parallel assemblies could also form cylindrin-like structures, such as those previously modeled (*27*, *46*). In fact, strong evidence for the extreme polymorphism of amyloid oligomers suggests that cylindrin-like assemblies could exist in a variety of structures with a variety of properties, including varying stabilities and toxicities (*39*, *44*).

References and Notes

1. B. Caughey, P. T. Lansbury Jr., *Annu. Rev. Neurosci.* **26**, 267 (2003).
2. W. F. Xue *et al.*, *J. Biol. Chem.* **284**, 34272 (2009).
3. R. Kodali, R. Wetzel, *Curr. Opin. Struct. Biol.* **17**, 48 (2007).
4. M. D. Kirkitadze, G. Bitan, D. B. Teplow, *J. Neurosci. Res.* **69**, 567 (2002).
5. R. Kayed *et al.*, *Science* **300**, 486 (2003).
6. G. Bitan, E. A. Fradinger, S. M. Spring, D. B. Teplow, *Amyloid* **12**, 88 (2005).
7. C. G. Glabe, *J. Biol. Chem.* **283**, 29639 (2008).
8. F. Chiti, C. M. Dobson, *Annu. Rev. Biochem.* **75**, 333 (2006).
9. F. Chiti, C. M. Dobson, *Nat. Chem. Biol.* **5**, 15 (2009).
10. J. C. Rochet, P. T. Lansbury Jr., *Curr. Opin. Struct. Biol.* **10**, 60 (2000).
11. R. Kayed *et al.*, *Mol. Neurodegener.* **2**, 18 (2007).
12. J. Horwitz, *Proc. Natl. Acad. Sci. U.S.A.* **89**, 10449 (1992).
13. S. Jehle *et al.*, *Proc. Natl. Acad. Sci. U.S.A.* **108**, 6409 (2011).
14. H. Ecroyd, J. A. Carver, *Cell. Mol. Life Sci.* **66**, 62 (2009).
15. S. Meehan *et al.*, *J. Mol. Biol.* **372**, 470 (2007).
16. A. Laganowsky *et al.*, *Protein Sci.* **19**, 1031 (2010).
17. M. J. Thompson *et al.*, *Proc. Natl. Acad. Sci. U.S.A.* **103**, 4074 (2006).
18. L. Goldschmidt, P. K. Teng, R. Riek, D. Eisenberg, *Proc. Natl. Acad. Sci. U.S.A.* **107**, 3487 (2010).
19. M. R. Sawaya *et al.*, *Nature* **447**, 453 (2007).
20. F. Sarsoza *et al.*, *Acta Neuropathol.* **118**, 505 (2009).
21. A. V. Kajava, U. Baxa, A. C. Steven, *FASEB J.* **24**, 1311 (2010).
22. J. Greenwald, R. Riek, *Structure* **18**, 1244 (2010).
23. B. M. Austen *et al.*, *Biochemistry* **47**, 1984 (2008).
24. P. Picone *et al.*, *Biophys. J.* **96**, 4200 (2009).
25. M. F. Engel *et al.*, *Proc. Natl. Acad. Sci. U.S.A.* **105**, 6033 (2008).
26. L. Khemtémourian, M. F. Engel, R. M. Liskamp, J. W. Höppener, J. A. Killian, *Biochim. Biophys. Acta* **1798**, 1805 (2010).
27. P. M. Pryciak, J. D. Conway, F. A. Eiserling, D. Eisenberg, in *Protein Structure, Folding, and Design*, D. L. Oxender, Ed. (Alan R. Liss, New York, 1986), vol. 39, pp. 243–246.
28. F. R. Salemme, D. W. Weatherford, *J. Mol. Biol.* **146**, 119 (1981).
29. F. R. Salemme, D. W. Weatherford, *J. Mol. Biol.* **146**, 101 (1981).
30. Y. Shafrir, S. Durell, N. Arispe, H. R. Guy, *Proteins* **78**, 3473 (2010).
31. J. D. Conway, thesis, UCLA (1986).
32. R. Nelson *et al.*, *Nature* **435**, 773 (2005).
33. A. G. Murzin, A. M. Lesk, C. Chothia, *J. Mol. Biol.* **236**, 1369 (1994).
34. T. L. Benzinger *et al.*, *Proc. Natl. Acad. Sci. U.S.A.* **95**, 13407 (1998).
35. R. Tycko, *Annu. Rev. Phys. Chem.* **62**, 279 (2011).
36. N. B. Last, E. Rhoades, A. D. Miranker, *Proc. Natl. Acad. Sci. U.S.A.* **108**, 9460 (2011).
37. J. W. Wu *et al.*, *J. Biol. Chem.* **285**, 6071 (2010).
38. K. Kar, M. Jayaraman, B. Sahoo, R. Kodali, R. Wetzel, *Nat. Struct. Mol. Biol.* **18**, 328 (2011).
39. S. Chimon *et al.*, *Nat. Struct. Mol. Biol.* **14**, 1157 (2007).
40. K. Ono, M. M. Condron, D. B. Teplow, *Proc. Natl. Acad. Sci. U.S.A.* **106**, 14745 (2009).
41. J. L. Tomic, A. Pensalfini, E. Head, C. G. Glabe, *Neurobiol. Dis.* **35**, 352 (2009).
42. Y. Yoshiike, R. Kayed, S. C. Milton, A. Takashima, C. G. Glabe, *Neuromolecular Med.* **9**, 270 (2007).
43. S. L. Bernstein *et al.*, *Nat. Chem.* **1**, 326 (2009).
44. M. Ahmed *et al.*, *Nat. Struct. Mol. Biol.* **17**, 561 (2010).
45. G. Bitan, S. S. Vollers, D. B. Teplow, *J. Biol. Chem.* **278**, 34882 (2003).
46. H. Jang *et al.*, *J. Mol. Biol.* **404**, 917 (2010).
47. H. A. Lashuel, D. Hartley, B. M. Petre, T. Walz, P. T. Lansbury Jr., *Nature* **418**, 291 (2002).
48. C. Liu *et al.*, *J. Am. Chem. Soc.* **133**, 6736 (2011).
49. V. A. Streltsov, J. N. Varghese, C. L. Masters, S. D. Nuttall, *J. Neurosci.* **31**, 1419 (2011).
50. F. C. Dehle, H. Ecroyd, I. F. Musgrave, J. A. Carver, *Cell Stress Chaperones* **15**, 1013 (2010).

Acknowledgments: We thank L. Goldschmidt for the 3D profile scan of ABC; J.-P. Colletier, D. Anderson, G. Fujii, J. Stroud, H. Chang, S. Sievers, J. Weissman, J. L. P. Benesch, G. Hochberg, and C. V. Robinson for useful discussion; J. Navarro at the UCLA Crystallization Facility; A. Berk and D. Guo for help with tissue culture experiments; and C. Ralston at the Advanced Light Source (ALS) 8.2.2 and K. Rajashankar and beamline staff at Argonne Photon Source (APS), Northeastern Collaborative Access Team beamlines 24-ID-E/C, for data collection. The last is supported by award RR-15301 from the National Center for Research Resources of the NIH. Use of the Advanced Photon Source, an Office of Science User Facility operated for the U.S. Department of Energy (DOE) Office of Science by Argonne National Laboratory, was supported by the U.S. DOE under contract no. DE-AC02-06CH11357. We thank the NIH Chemistry Biology Interface Training program (award 5T32GM008496) sponsorship for A.L., UCLA Dissertation Year fellowships awarded to A.L. and M.Z., NSF award MCB-0445429, NIH award 1R01-AG029430, award NIH-016570 from Alzheimer's Disease Research at UCLA, and HHMI for support. Atomic coordinates and structure factors have been deposited in the PDB with the following accession codes: K11V (3SGO), K11V-Br2 (3SGM), K11V-Br8 (3SGN), K11V^{V2L} (3SGP), K11V-TR (3SGR), and GDVIEV (3SGS). A11 is available under a uniform biological material transfer agreement with the University of California, Irvine. UCLA has filed a provisional patent on cylindrin as the possible generic etiologic agent of amyloid diseases.

Supporting Online Material

www.sciencemag.org/cgi/content/full/335/6073/1228/DC1
Materials and Methods
SOM Text
Figs. S1 to S11
Tables S1 to S4
References (*51*–*82*)

25 August 2011; accepted 5 January 2012
10.1126/science.1213151